# I-7. Probabilistic Stability Analysis (Reliability Analysis)

## Key Concepts

Sliding stability analysis of concrete or embankment dams does not lend itself well to the event tree method in all cases, particularly under normal operating conditions. That is because stability, or lack thereof, results from an interaction between the applied loads, the pore pressures or uplift forces, and the shear strength. There is typically not a linear step-by-step progression for these factors, although changes in shear strength and/or drainage may occur with time. Therefore, it is helpful to obtain some numerical information about the probability of failure (or unsatisfactory performance). This information can be used to estimate a range in the probability of sliding for event tree nodes (see section on Event Trees) representing various loading conditions.

The traditional factor of safety approach provides some insight into failure probability; typically conservative input values (shear strength and water pressures) are used in the analyses, and if the resulting factor of safety satisfies established criteria, the likelihood of failure is low. How low is another question, and factor of safety by itself is not a good indication. This is seen in Figure I-7-1, which shows the distributions of driving force and resisting force for two cases.

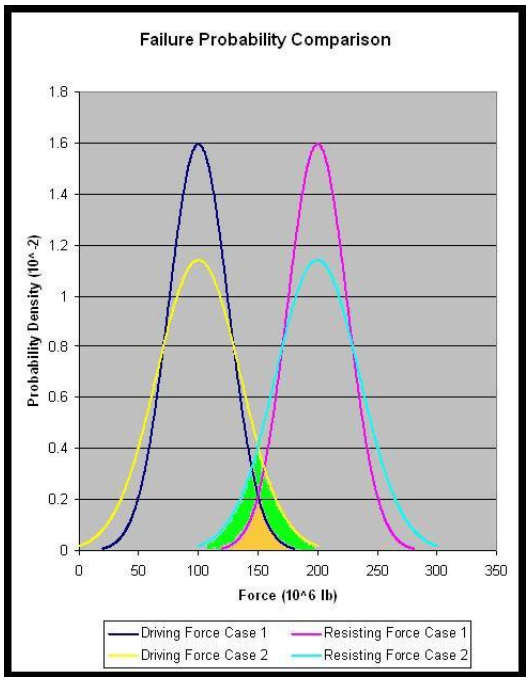


**Figure I-7-1. Factor of Safety and Failure Probability Comparison. For each case, the distance between the peaks can be thought of as a measure of the safety factor, whereas the failure probability is proportional to the size of the overlap area.**

The mean factor of safety (mean resisting force divided by mean driving force) is exactly the same for both cases. However, the probability of failure (area under curves where the driving force is greater than the resisting force) is twice as high for the yellow and light blue curves (i.e. the orange area plus the green area) than it is for the dark blue and lavender curves (orange area).

With the availability of commercial computer analysis tools; now, if you can program a deterministic analysis into a spreadsheet, you can use it to perform probabilistic analyses. This section describes the basic concepts of performing probabilistic analyses using a standard spreadsheet program (Microsoft ® Excel) and commercially available macro add-ins for probabilistic analysis (Palisade Corporation's Decision Tools Suite which includes @Risk). Other companies sell similar software (e.g. Lotus 1-2-3, and Crystal Ball by Decisioneering, Inc.). It should be noted that other analysis programs have the capability to perform some probabilistic analysis (e.g. GRAVDAM for concrete gravity dams and SLOPE/W for embankment dams). However, these programs may not have the capability to display the sensitivity rank coefficients as described later, and hence some additional judgment may be needed when using these programs to perform sensitivity analyses. In addition, SLOPE/W will indicate a probability of failure equal to zero if none of the Monte-Carlo calculated factors of safety are less than 1.0. A reliability index is provided, but it is not clear what type of distribution is assumed in its calculation. GRAVDAM incorporates a cracked base analysis that must be used with caution (see also section on Concrete Gravity Dams).

Using the Monte Carlo approach, the standard deterministic equations for calculating the factor of safety are programmed into a spreadsheet, but instead of defining the input parameters as single constant values, they are defined as distributions of values. Thus, instead of calculating a single value for the output factor of safety, a distribution of safety factors is generated from numerous Monte Carlo trials, whereby each of the input distributions are sampled in a manner consistent with their shape for each iteration. This output distribution is used to determine the probability of the safety factor being less than the threshold value representing failure or unsatisfactory performance.

For the purposes of this section of the manual, the probability of unsatisfactory performance is defined as the probability of a factor of safety (FS) less than 1.0. However, other threshold values can be used (or the results tempered with judgment). For example, if the dam is particularly susceptible to deformation damage, a larger value of safety factor may appropriately define the state at which "unsatisfactory performance" occurs (El-Ramly et al, 2002), and the probability of being below that value is calculated.

# Example: Embankment Post-Liquefaction Stability

Consider the homogeneous embankment dam geometry shown in Figure I-7-2. The dam is in a seismically active area. What appears to be a continuous clean sand layer, approximately four to six feet thick, was encountered in three borings, approximately eight feet below the dam-foundation contact. The minimum corrected $(N_1)_{60}$ blow count values encountered in this layer varied from 13 to 15 depending on the boring. The toe of the dike is wet, indicating a high phreatic surface and saturated foundation materials in that area. Piezometers installed in the embankment indicate differences in the phreatic surface of about nine feet from one hole to another at the same distance downstream of

the centerline. Given that the sand layer liquefies, what is the probability of post-liquefaction instability?

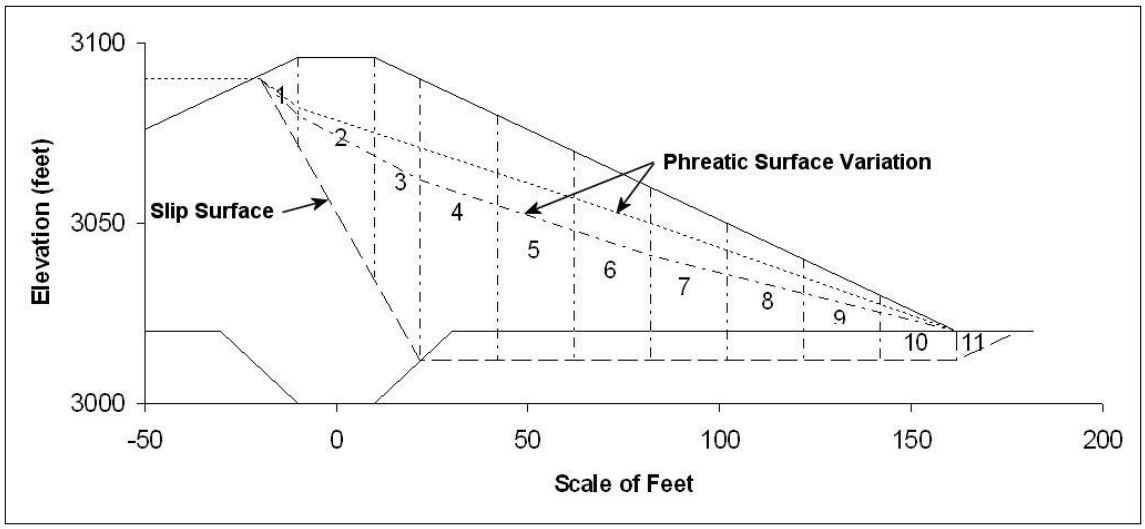


**Figure I-7-2. Example Embankment Dam Geometry**

The critical sliding surface was assumed to follow the liquefied sand layer and intersect the upstream face below the reservoir surface at normal full pool, such that no embankment remnant would be left to retain the reservoir. Although there may be slip surfaces with a lower factor of safety, some of them may not be critical in the sense that a crest remnant capable of retaining the reservoir remains. It may be appropriate to examine other slip surfaces, or use a factor of safety greater than 1.0 to represent unsatisfactory performance to cover the possibility of a more critical slip surface. The simplified Bishop method of analysis (Scott, 1974) was programmed into a spreadsheet, as shown in Figure I-7-3. The "allow circular reference" feature in Excel is used to iterate to the solution. Eleven slices were used to define the potential sliding mass.

| | A | B | C | D | E | F | G | H | I | J | K | L |
|---|---|---|---|---|---|---|---|---|---|---|---|---|
| 1 | Bishop's Slope Stability Analysis | | | | | | | | | | | |
| 2 | | | | | | | | | | | | |
| 3 | Drained Strengths | | | Undrained Strengths | | | Density | | | | | |
| 4 | c' = | 696 | psf | c = | 637 | psf | γ = | 114 | pcf | | | |
| 5 | tan Φ' = | 0.672 | | tan Φ = | 0 | | | | | | | |
| 6 | Φ' = | 33.9 | degrees | Φ = | 0 | | | | | | | |
| 7 | | | | | | | | | | | | |
| 8 | | | | | | | | | | | | |
| 9 | Slice | Δxi | c*Δxi | ui | ui*Δxi | Wi | θi | (Wi-ui*Δxi)*tanΦ | C + H | cos(θi)*[1+(tanθi*tanΦ/FS)] | I / J | Wi*sinθi |
| 10 | | (ft) | (kips) | (ksf) | (kips) | (kips) | (deg) | (kips) | | | | (kips) |
| 11 | | | | | | | | | | | | |
| 12 | 1 | 12 | 8.35 | 0.28 | 3.37 | 17.72 | 60.6 | 9.64 | 18.00 | 0.92 | 19.63 | 15.44 |
| 13 | 2 | 20 | 13.92 | 1.45 | 29.02 | 99.97 | 60.6 | 47.68 | 61.60 | 0.92 | 67.21 | 87.10 |
| 14 | 3 | 12 | 8.35 | 2.90 | 34.82 | 94.06 | 60.6 | 39.81 | 48.16 | 0.92 | 52.55 | 81.95 |
| 15 | 4 | 20 | 12.73 | 0 | 0.00 | 165.86 | 0.0 | 0.00 | 12.73 | 1.00 | 12.73 | 0.00 |
| 16 | 5 | 20 | 12.73 | 0 | 0.00 | 143.14 | 0.0 | 0.00 | 12.73 | 1.00 | 12.73 | 0.00 |
| 17 | 6 | 20 | 12.73 | 0 | 0.00 | 120.42 | 0.0 | 0.00 | 12.73 | 1.00 | 12.73 | 0.00 |
| 18 | 7 | 20 | 12.73 | 0 | 0.00 | 97.70 | 0.0 | 0.00 | 12.73 | 1.00 | 12.73 | 0.00 |
| 19 | 8 | 20 | 12.73 | 0 | 0.00 | 74.98 | 0.0 | 0.00 | 12.73 | 1.00 | 12.73 | 0.00 |
| 20 | 9 | 20 | 12.73 | 0 | 0.00 | 52.26 | 0.0 | 0.00 | 12.73 | 1.00 | 12.73 | 0.00 |
| 21 | 10 | 20 | 12.73 | 0 | 0.00 | 29.54 | 0.0 | 0.00 | 12.73 | 1.00 | 12.73 | 0.00 |
| 22 | 11 | 16 | 11.13 | 0.19 | 3.00 | 7.27 | -26.6 | 2.87 | 14.01 | 0.68 | 20.74 | -3.26 |
| 23 | | | | | | | | | | Sum -> | 249.26 | 181.23 |
| 24 | FS = ΣK/ΣL = | 1.38 | | | | | | | | | | |

**Figure I-7-3. Bishops Method of Slope Stability Analysis**

Input variables defined as distributions include: (1) embankment soil unit weight ($\gamma$), (2) effective stress cohesion of the embankment material (c'), (3) effective stress friction angle of the embankment material ($\varphi$'), (4) undrained residual shear strength of the liquefied sand layer ($S_u$), and (5) water forces at the base of each embankment slice for which effective stress parameters were defined. No test results were available for the embankment materials. Therefore, the mean, standard deviation, maximum, and minimum values listed in *Design of Small Dams* (BOR, 1987) for SC material (see Table I-7-1) were used to define truncated normal distributions. Normal distributions are often truncated because the standard normal distribution is unbounded which can result in negative values that may not make sense. The @Risk function for the effective stress cohesion, for example, is:

RiskNormal(720,360,RiskTruncate(101,1224)).

The friction angles were converted to tan $\varphi$' for the spreadsheet calculations. It should be noted that in many cases these types of embankment materials are treated as undrained, or "friction only" strengths are used based on the shear strength curves. It should also be noted that the strength values from *Design of Small* Dams likely came from tests on compacted laboratory samples and may not be totally representative of saturated embankment conditions. However, both c' and $\varphi$' from *Design of Small* Dams are used in this example for illustration purposes.

**Table I-7-1. Summary of embankment input properties**

| Property | Minimum | Maximum | Mean | Standard Deviation |
|---|---|---|---|---|
| Moist Unit Weight ($lb/ft^3$) | 91.1 | 131.8 | 115.6 | 14.1 |
| c' ($lb/ft^2$) | 101 | 1224 | 720 | 360 |
| $\varphi$' (degrees) | 28.4 | 38.3 | 33.9 | 2.9 |

For simplicity, moist soil unit weight was used for the entire soil mass, including the foundation alluvium. It is recognized that the saturated embankment unit weight (below the phreatic surface) will actually be slightly higher, and the alluvial materials could also be somewhat different. It is also assumed that the effective stress parameters listed in Table I-7-1 are equally applicable above and below the phreatic surface.

A variation in phreatic surface of up to nine feet was used to estimate pore pressures and forces at the base of each slice where the sliding surface passes through the embankment, as shown in Figure I-7-2. A uniform distribution between the upper and lower values of pore pressure (in $kips/ft^2$) was assigned, in this case RiskUniform(1.22,1.68), indicating any value between the upper and lower value is equally likely.

Finally, undrained residual shear strength of the liquefied foundation sand was estimated using the curves developed by Seed and Harder (Seed et al, 2003). Upper and lower bound curves are provided as a function of corrected blow count. It was assumed that a strength midway between the curves represented the best estimate value. A triangular distribution between the upper and lower bound values, with a peak at the best estimate value, was used to define this input parameter, RiskTriang(360,630,920) in $lb/ft^2$. It is recognized that more recent guidance on the selection of residual strengths exists, but it is

expected the Seed and Harder relationship would be slightly more conservative, and for simplicity and illustration purposes it was used alone.

After entering the input distributions in the spreadsheet cells, the factor of safety cell is selected as the output and the simulation settings are adjusted. In this case, 10,000 iterations were specified. For each iteration, the input distributions are sampled in a manner consistent with their shape or probability density function, and an individual factor of safety is calculated. This results in a record of the calculated factors of safety for the entire simulation. It is a simple matter to sort the output factors of safety in ascending or descending order using the "sort" command of the spreadsheet program. The probability of FS<1.0 is taken as the number of iterations with calculated factor of safety less than 1.0 divided by the total number of iterations. In this case, 228 iterations produced a factor of safety less than 1.0. Therefore, the estimated probability of FS<1.0 is 228/10,000 or 0.0228.

To help understand which input distributions have the greatest effect on the results, the @Risk program prints out a list of ranking coefficients. Those input distributions with the highest positive or negative ranking coefficients affect the results most. For the example just described, the coefficients are shown in Table I-7-2. It can be seen that the drained cohesion of the embankment, c', and the undrained residual shear strength of the sand layer, $S_u$, affect the results the most. A negative ranking coefficient just means that the variable is negatively correlated with the result. For example, an increase in pore pressure results in a decrease in factor of safety, as expected.

**Table I-7-2. Embankment dam sensitivity rank coefficients**

| Rank | Name | Cell | Regression | Correlation |
|---|---|---|---|---|
| **1** | c' | $B$4 | 0.726344 | 0.732725132 |
| **2** | $S_u$ | $E$4 | 0.590719261 | 0.575407848 |
| **3** | γ | $H$4 | -0.292465055 | -0.272376816 |
| **4** | φ' | $B$5 | 0.137192535 | 0.130003719 |
| **5** | u slice 2 | $D$13 | -0.072522808 | -0.070526537 |
| **6** | u slice 3 | $D$14 | -0.052556307 | -0.051631753 |
| **7** | u slice 11 | $D$22 | -0.020666858 | -0.020920598 |
| **8** | u slice 1 | $D$12 | -0.018467738 | -0.004675745 |

Although probabilistic analyses attempt to account for uncertainty, when dealing with dam safety engineering applications, there may not be sufficient data to define the input distributions with confidence. Therefore, it may be appropriate to perform sensitivity studies using variations to the input distributions. For the case of the embankment slope described above, two additional simulations were run with the following variations:

- Examination of test values for SM soils from *Design of Small Dams* (BOR, 1987) indicates a higher mean and more variation in c' than for SC material. Since some siltier zones were observed in the embankment during sampling, more variation in this parameter may be warranted. However, the mean value used appears to be appropriate. The standard deviation of the drained embankment cohesion, c', was increased by 50 percent to 540 lb/ft$^2$. In addition, rather than truncating the maximum and minimum values for c' at the soil test values shown in Table I-7-1, these values were allowed to vary between 20 and 2000 lb/ft$^2$ to

account for the fact that the full range of possible values may not have been captured by the limited testing.

- For the second sensitivity analysis, the undrained residual strength of the sand layer was taken as RiskTriang(310,560,790) based on an $(N_1)_{60}$ value of 13 (lower value from the exploration) rather than 14 (mid-range value).

The results of all three simulations are summarized in Table I-7-3. Increasing the standard deviation and upper limit for c' also increased the location of the output distribution centroid, resulting in a higher mean factor of safety. However, although the mean factor of safety increased when more variation was allowed, the probability of FS<1.0 also increased. This is the phenomenon illustrated in Figure I-7-1. Decreasing the residual undrained shear strength of the sand layer decreased the mean factor of safety and also increased the probability of FS<1.0, as expected. These analyses provide a quantitative indication of what variation in the inputs actually means in terms of failure likelihood for the embankment studied. They also provide an indication of the likely range of failure probability, given uncertainty in the input parameters. It should be noted that even if the embankment remains stable, deformations could result in transverse cracking through which seepage erosion could take place. This must also be considered in evaluating the overall risks posed by the dam and reservoir.

**Table I-7-3. Results of embankment post-liquefaction simulations**

| Case | Mean F.S. | Probability F.S.<1.0 |
|---|---|---|
| Original Input Distributions | 1.38 | 0.0228 |
| Increase Std Dev and bounds of c' | 1.44 | 0.0345 |
| Lower the best estimate and bounds for Undrained Residual Strength | 1.32 | 0.0605 |

# Example RCC Gravity Dam Stability

The probabilistic method is equally applicable to sliding of concrete structures. For example, construction of a 160-foot-high roller-compacted concrete (RCC) gravity dam in a wide canyon was suspended for winter shut down after the RCC reached a height of 20 feet. The following construction season, the cold joint surface of the previous year was thoroughly cleaned and coated with mortar, and the remainder of the dam was placed. A gallery was constructed such that the gallery floor would be about 5 feet above tailwater during PMF conditions. A line of three-inch-diameter drains, spaced at 10 feet, was angled downstream from the gallery, intersecting the cold joint about 28 feet downstream of the axis. Although a 3.5-foot-high parapet wall was constructed on the upstream side of the dam crest, the spillway was sized to pass the probable maximum flood (PMF) without encroaching on the wall. Due to concerns about the strength of the cold joint, five six-inch diameter cores were taken one year later. Two of the five cores were not bonded at the lift joint. The remaining three were tested in direct shear at varying normal stresses. Although only three data points were generated, the results were well behaved as shown in Figure I-7-4. Accounting for about 40 percent de-bonded area of the joint, it was determined that the design intent was still met. Several years later, the PMF was revised and a flood-frequency analysis was performed. Although the new PMF did not overtop the dam, it encroached about 2.3 feet onto the parapet wall. Maximum

tailwater did not change significantly. Additional stability analyses were undertaken to evaluate the likelihood of failure under the new loading condition.

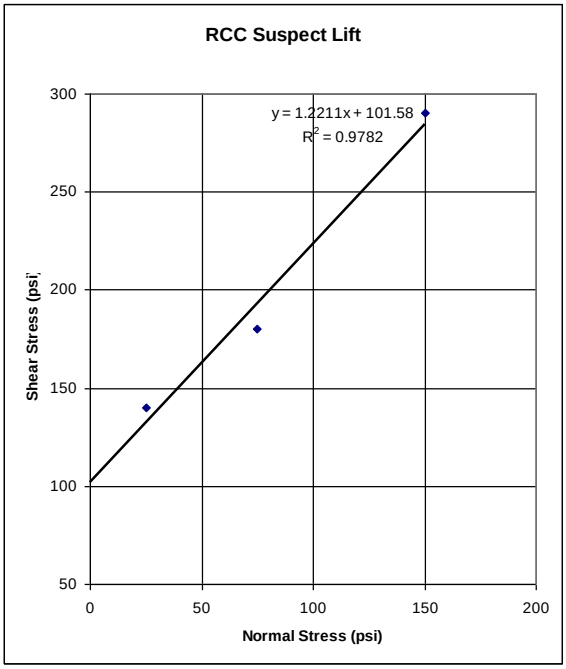


**Figure I-7-4. Direct shear test results for suspect RCC lift joint**

The dam cross section shown in Figure I-7-5 was used in the analysis. The vertical stress at the upstream face is calculated considering the standard equation from mechanics of materials: P/A ± Mc/I to account for the vertical load (P) and the moment (M) induced by the reservoir for the combined stress condition, as indicated by Watermeyer (2006). Initially, uplift along the cold joint is approximated by a bi-linear distribution of pressures, varying from full reservoir pressure at the upstream face, to a reduced pressure at the line of drains, to tailwater at the downstream face. The total head at the line of drains is defined as $F_d$ * (Reservoir El. – Tailwater El.) + Tailwater El., where $F_d$ is the drain factor (1-efficiency). The pressure head is determined by subtracting the elevation of the potential sliding surface from the total head, and the pressure head is converted to an uplift pressure for analysis. The effective stress is calculated along the potential sliding plane by subtracting the uplift pressure from the total stress, and where the effective stress is calculated to be tensile, no resistance is included for that portion of the plane. Since the locations of potential joint de-bonding are unknown, the cold joint was also assumed to be cracked to the point of zero effective stress in this case. Full reservoir pressure was assumed in the crack until it extended past the drains. Then, approximate equations were used to adjust the drain factor to account for the crack length, based on research performed at the University of Colorado (Amadei et al, 1991). These equations require the "allow circular reference" feature of Excel to iterate on a crack length. The factor of safety was then calculated from the familiar equation FS = [c'A + (W-U)tanφ']/D, where W is the vertical load, A is the bonded area, U is the uplift force, and D is the driving force taking into account both the downstream-directed reservoir load and the upstream-directed tailwater load.

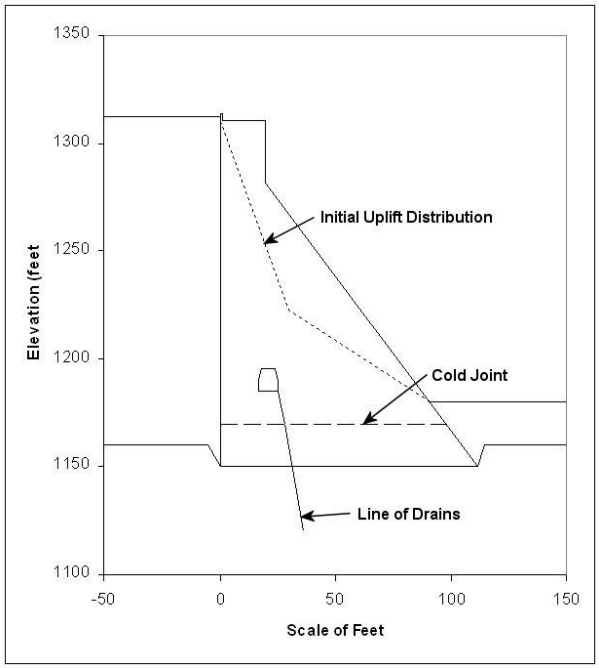


**Figure I-7-5. Cross-sectional geometry of an RCC gravity dam**

The equations for limit equilibrium analysis were programmed into a spreadsheet. Input variables that were defined as distributions included the following: (1) drain factor $F_d$, (2) tangent of the intact friction angle on the potentially weak lift joint φ', (3) intact cohesion on the potentially weak lift joint c', (4) percentage of the joint that is intact, and (5) the RCC unit weight. Table I-7-4 defines the distributions that were used.

**Table I-7-4. Summary of concrete input properties**

| Property | Distribution | Minimum | Mode | Maximum |
|---|---|---|---|---|
| Initial Drain Factor, $F_d$ | Uniform | 0.33 | n/a | 0.75 |
| φ' (degrees) | Triangular | 43 | 50 | 57 |
| Intact c' ($lb/in^2$) | Triangular | 50 | 100 | 150 |
| Percent Intact | Triangular | 43 | 60 | 71 |
| Unit Weight ($lb/ft^3$) | Uniform | 146 | n/a | 152 |

The RCC unit weight, based on measurements from the core samples, had only limited variability, and a uniform distribution between the minimum and maximum measured values was used. For the other parameters:

- The initial drain factor was taken to be a uniform distribution based on piezometer measurements and experience with other concrete dams of similar geometry.
- The coring would suggest that about 60 percent of the lift surface was bonded, assuming the cores were not mechanically broken at that elevation during drilling. To estimate a likely range, the percentage was adjusted by assuming the drilling of two more holes yielded bonded lifts (upper bound estimate), or yielded unbonded lifts (lower bound estimate).

- Both the cohesion and tangent friction angle were defined as triangular distributions, with the peak or mode of the distribution estimated using the straight line fit shown in Figure I-7-4. High and low values were estimated based on experience with other direct shear tests on concrete joints, and interpolating other reasonable lines through the data points.

The minimum safety factor calculated from 10,000 iterations was 1.43, with a mean value of 2.42. The sensitivity analysis indicated the cohesion had the largest effect on the results as shown in Table I-7-5.

**Table I-7-5. RCC dam sensitivity rankings**

| Rank | Name | Cell | Regression | Correlation |
|---|---|---|---|---|
| 1 | Intact Cohesion (psi) = | $B$17 | 0.759017659 | 0.759702063 |
| 2 | TAN Friction Angle = | $B$16 | 0.411501707 | 0.395787559 |
| 3 | Percent Intact = | $B$18 | 0.368619688 | 0.349212338 |
| 4 | Drain Factor = | $B$15 | -0.311968848 | -0.314501945 |
| 5 | Concrete Density (pcf) = | $B$19 | 0.09730957 | 0.085434774 |

Figure I-7-4 suggests that the cohesion and friction angle are negatively correlated. That is, as the friction angle becomes greater, a line that passes through the data would intercept the vertical axis at a lower cohesion value, and vice versa. @Risk allows the user to correlate input variables, such that in this case, a high value of cohesion will only be sampled with a low value of friction angle, and vice versa. Since there were limited data points upon which to base a correlation, a negative correlation coefficient of 0.8 was selected, meaning that the highest cohesion value doesn't have to be associated with the absolute lowest friction angle, but the general trend of the correlation is maintained. The minimum factor of safety calculated with this correlation is 1.79, higher than if the correlation is not maintained, indicating that ignoring the correlation would be conservative.

Since the factor of safety never drops below 1.0 in any of the Monte Carlo trials, it is not possible to determine the probability of FS<1.0 in the same manner as for the embankment dam example. Based on the fact that none of the 10,000 iterations produced a FS<1.0, it can only be said that the probability of FS<1.0 is less than 1 in 10,000. In some (but not all) cases, this upper bound of failure probability can be improved upon by performing more Monte Carlo trials. However, it is also possible to estimate a probability of FS<1.0 by fitting a distribution to the results.

For this, the parameter "reliability index" or β must be introduced. The reliability index is simply the "number of standard deviation units" between the mean value and the value representing failure. Figure I-7-6 shows the output factor of safety distribution for the first case discussed for the RCC gravity dam; with cohesion and friction angle treated as independent of each other. Goodness of fit tests indicate the distribution follows a normal (bell-shaped) distribution quite well. The reliability index in this case, relative to a safety factor of 1.0, is $(FS_{AVG} - 1.0)/\sigma_F$, where $FS_{AVG}$ is the mean safety factor and $\sigma_F$ is the standard deviation of the safety factor distribution, or $\beta = (2.425\text{-}1.0)/0.3126 = 4.56$. There is a standard function in Microsoft Excel that allows one to estimate the probability of FS<1.0 directly from the reliability index, which is 1-NORMSDIST(β). In this case, using this function produces a probability of FS<1.0 of $2.61 \times 10^{-6}$. This is a very low number, which seems reasonable given the high mean factor of safety and the fact that

the minimum value calculated in 10,000 iterations never dropped below 1.4. In many cases, the output factors of safety may not follow a normal distribution, but rather a lognormal distribution. This same method can be used to estimate the probability of FS<1.0. The only difference is that the reliability index is calculated with a different formula (Scott et al, 2001), as follows:

$$\beta_{\log normal} = \frac{\ln\left(\frac{FS_{mean}}{\sqrt{1+V_{FS}^2}}\right)}{\sqrt{\ln\left(1+V_{FS}^2\right)}}$$

Where $FS_{mean}$ is the average factor of safety and $V_{FS}$ is the coefficient of variation for the factor of safety, equal to the standard deviation divided by the mean.

Note: for very long potential failure surfaces through a given material, the strength parameters may not be consistent all along the surface. The "spatial variability" can be accounted for by dividing the surface into representative segments (perhaps based on spacing of test information) and defining separate input distributions for each segment.

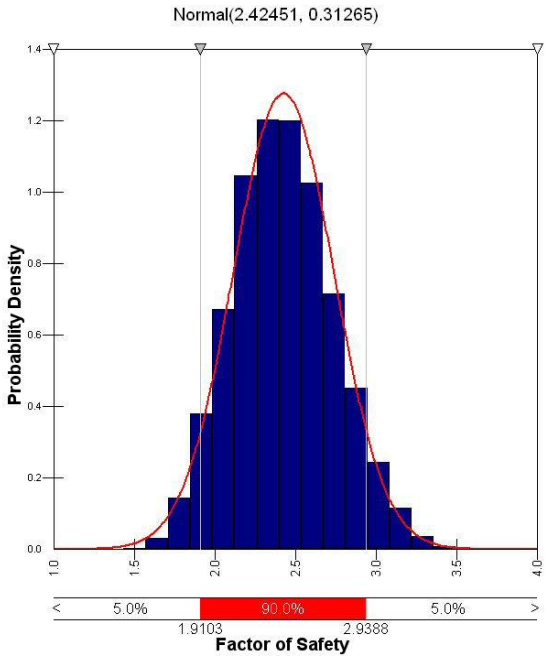


**Figure I-7-6. Output factor of safety distribution for RCC dam with a fitted normal distribution superimposed**

# Using Reliability Analysis within a Risk Analysis

The type of probabilistic stability analysis described in the preceding paragraphs is sometimes referred to as "reliability analysis". Reliability analysis is typically not used as the sole method for estimating failure probability, and the results of such analysis must be moderated using engineering judgment. However, when appropriate models are available, they can be a useful tool in estimating response components or "conditional" probabilities (probabilities that are conditional upon given loadings or states). That is,

given the loading condition (e.g. reservoir level or earthquake) and state (e.g. liquefied foundation), they can help a team estimate the occurrence probability of a particular event of a Potential Failure Mode (PFM). For example, initiation of sliding (e.g. FS<1.0) may not equate to failure. Other events may also need to occur as captured in an event tree. Reliability analysis has been used as a tool in the risk analyses for a variety of structures, including Folsom Dam (concrete gravity), Upper Stillwater Dam (RCC gravity dam), Pueblo Dam (concrete buttress dam), Gibson Dam (concrete arch dam), and Horse Mesa Dam (concrete arch dam), as well as for estimating construction risks with an excavation at the toe of Mormon Island Auxiliary Dam (embankment).

# Model Uncertainty

The preceding discussion provides a method for calculating probabilities considering uncertainties in the input parameters. This type of uncertainty is sometimes referred to as parameter uncertainty. However, significant uncertainty also exists as to how well the models used in the calculations actually reflect the real situation. This is sometimes referred to as model uncertainty. Models are just that, limited approximations. Vick (2002) provides additional discussion concerning the limitations of models. The models used in the spreadsheet calculations previously described are two-dimensional simplifications of complex three-dimensional problems (e.g. the equation used in the RCC dam example does not take into account shear resistance along the sides of the critical section). It may be appropriate to interpret the results of the numerical reliability analyses based on subjective degree of belief considerations (see Section on Subjective Probability and Expert Elicitation). For example, if there are significant three-dimensional effects that tend to help with stability, but a complex three-dimensional analysis cannot be easily programmed into a spreadsheet, the calculated failure probability can be reduced based on the expectation of beneficial 3-D effects. Similarly, if there are uncertainties in the model with the potential to make things one-sidedly worse, such as the possibility that shear strengths will not be mobilized at the same shear strains for different materials along the sliding plane, the failure probability can be increased over the calculated value.

# Exercise

Given a mean calculated factor of safety of 1.46 with a standard deviation of 0.26 and a standard normal distribution, what is the probability of a factor of safety of less than 1? What would be the probability be with a standard deviation of 0.16?

See the attached chart and Z-table for normal distribution. Note that Z is equivalent to the Excel function NORMSDIST($\beta$).

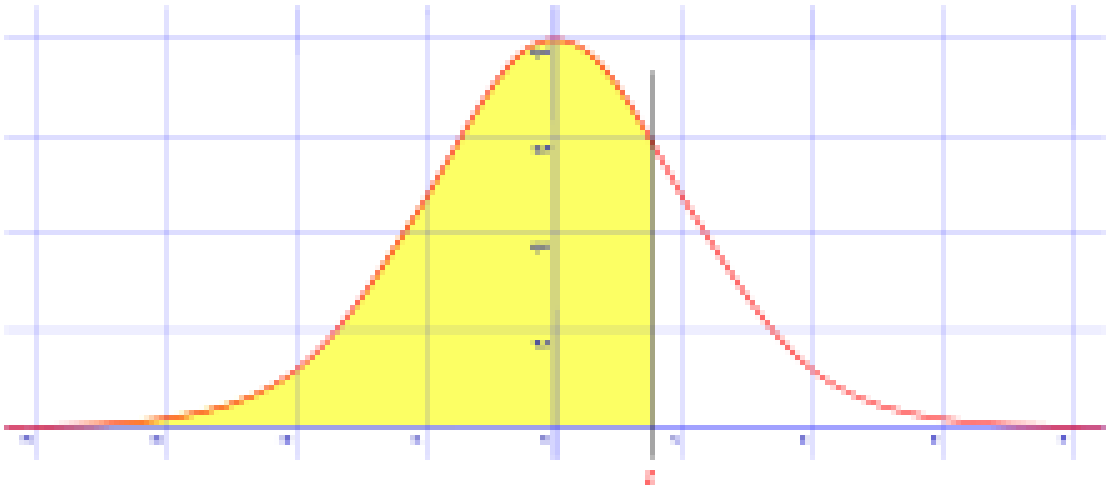

This table gives a probability that the outcome or sampled value of a normally distributed random variable is less than Z. Using the table: for example, for a Z of 1.56 read down the left column to 1.5 then across to 0.06.

| *z* | **0.00** | **0.01** | **0.02** | **0.03** | **0.04** | **0.05** | **0.06** | **0.07** | **0.08** | **0.09** |
|---|---|---|---|---|---|---|---|---|---|---|
| **0.0** | 0.5000 | 0.5040 | 0.5080 | 0.5120 | 0.5160 | 0.5199 | 0.5239 | 0.5279 | 0.5319 | 0.5359 |
| **0.1** | 0.5398 | 0.5438 | 0.5478 | 0.5517 | 0.5557 | 0.5596 | 0.5636 | 0.5675 | 0.5714 | 0.5753 |
| **0.2** | 0.5793 | 0.5832 | 0.5871 | 0.5910 | 0.5948 | 0.5987 | 0.6026 | 0.6064 | 0.6103 | 0.6141 |
| **0.3** | 0.6179 | 0.6217 | 0.6255 | 0.6293 | 0.6331 | 0.6368 | 0.6406 | 0.6443 | 0.6480 | 0.6517 |
| **0.4** | 0.6554 | 0.6591 | 0.6628 | 0.6664 | 0.6700 | 0.6736 | 0.6772 | 0.6808 | 0.6844 | 0.6879 |
| **0.5** | 0.6915 | 0.6950 | 0.6985 | 0.7019 | 0.7054 | 0.7088 | 0.7123 | 0.7157 | 0.7190 | 0.7224 |
| **0.6** | 0.7257 | 0.7291 | 0.7324 | 0.7357 | 0.7389 | 0.7422 | 0.7454 | 0.7486 | 0.7517 | 0.7549 |
| **0.7** | 0.7580 | 0.7611 | 0.7642 | 0.7673 | 0.7704 | 0.7734 | 0.7764 | 0.7794 | 0.7823 | 0.7852 |
| **0.8** | 0.7881 | 0.7910 | 0.7939 | 0.7967 | 0.7995 | 0.8023 | 0.8051 | 0.8078 | 0.8106 | 0.8133 |
| **0.9** | 0.8159 | 0.8186 | 0.8212 | 0.8238 | 0.8264 | 0.8289 | 0.8315 | 0.8340 | 0.8365 | 0.8389 |
| **1.0** | 0.8413 | 0.8438 | 0.8461 | 0.8485 | 0.8508 | 0.8531 | 0.8554 | 0.8577 | 0.8599 | 0.8621 |
| **1.1** | 0.8643 | 0.8665 | 0.8686 | 0.8708 | 0.8729 | 0.8749 | 0.8770 | 0.8790 | 0.8810 | 0.8830 |
| **1.2** | 0.8849 | 0.8869 | 0.8888 | 0.8907 | 0.8925 | 0.8944 | 0.8962 | 0.8980 | 0.8997 | 0.9015 |
| **1.3** | 0.9032 | 0.9049 | 0.9066 | 0.9082 | 0.9099 | 0.9115 | 0.9131 | 0.9147 | 0.9162 | 0.9177 |
| **1.4** | 0.9192 | 0.9207 | 0.9222 | 0.9236 | 0.9251 | 0.9265 | 0.9279 | 0.9292 | 0.9306 | 0.9319 |
| **1.5** | 0.9332 | 0.9345 | 0.9357 | 0.9370 | 0.9382 | 0.9394 | 0.9406 | 0.9418 | 0.9429 | 0.9441 |
| **1.6** | 0.9452 | 0.9463 | 0.9474 | 0.9484 | 0.9495 | 0.9505 | 0.9515 | 0.9525 | 0.9535 | 0.9545 |
| **1.7** | 0.9554 | 0.9564 | 0.9573 | 0.9582 | 0.9591 | 0.9599 | 0.9608 | 0.9616 | 0.9625 | 0.9633 |
| **1.8** | 0.9641 | 0.9649 | 0.9656 | 0.9664 | 0.9671 | 0.9678 | 0.9686 | 0.9693 | 0.9699 | 0.9706 |
| **1.9** | 0.9713 | 0.9719 | 0.9726 | 0.9732 | 0.9738 | 0.9744 | 0.9750 | 0.9756 | 0.9761 | 0.9767 |
| **2.0** | 0.9772 | 0.9778 | 0.9783 | 0.9788 | 0.9793 | 0.9798 | 0.9803 | 0.9808 | 0.9812 | 0.9817 |
| **2.1** | 0.9821 | 0.9826 | 0.9830 | 0.9834 | 0.9838 | 0.9842 | 0.9846 | 0.9850 | 0.9854 | 0.9857 |
| **2.2** | 0.9861 | 0.9864 | 0.9868 | 0.9871 | 0.9875 | 0.9878 | 0.9881 | 0.9884 | 0.9887 | 0.9890 |
| **2.3** | 0.9893 | 0.9896 | 0.9898 | 0.9901 | 0.9904 | 0.9906 | 0.9909 | 0.9911 | 0.9913 | 0.9916 |
| **2.4** | 0.9918 | 0.9920 | 0.9922 | 0.9925 | 0.9927 | 0.9929 | 0.9931 | 0.9932 | 0.9934 | 0.9936 |
| **2.5** | 0.9938 | 0.9940 | 0.9941 | 0.9943 | 0.9945 | 0.9946 | 0.9948 | 0.9949 | 0.9951 | 0.9952 |
| **2.6** | 0.9953 | 0.9955 | 0.9956 | 0.9957 | 0.9959 | 0.9960 | 0.9961 | 0.9962 | 0.9963 | 0.9964 |
| **2.7** | 0.9965 | 0.9966 | 0.9967 | 0.9968 | 0.9969 | 0.9970 | 0.9971 | 0.9972 | 0.9973 | 0.9974 |
| **2.8** | 0.9974 | 0.9975 | 0.9976 | 0.9977 | 0.9977 | 0.9978 | 0.9979 | 0.9979 | 0.9980 | 0.9981 |
| **2.9** | 0.9981 | 0.9982 | 0.9982 | 0.9983 | 0.9984 | 0.9984 | 0.9985 | 0.9985 | 0.9986 | 0.9986 |
| **3.0** | 0.9987 | 0.9987 | 0.9987 | 0.9988 | 0.9988 | 0.9989 | 0.9989 | 0.9989 | 0.9990 | 0.9990 |

## References


Amadei, B., T. Illangasekare, C. Chinnaswamy, D.I. Morris, "Estimating Uplift in Cracks in Concrete Dams," Proceedings, International Conference on Hydropower, Denver, Colrado, July 24-26, 1991.

Bureau of Reclamation, *Design of Small Dams*, Third Edition, Denver, CO, 1987.

El-Ramly, H., N.R. Morgenstern, and D.M. Cruden, "Probabilistic Slope Stability Analysis for Practice," *Canadian Geotechnical Journal*, NRC Canada, Volume 39, pp. 665-683, 2002.

Olson, S. M. & Stark, T. D, "Liquefied strength ratio from liquefaction case histories," Canadian Geotechnical Journal, Volume 39, No. 3, pp 629–647, March, 2002.

Seed, R.B., K.O. Cetin, R.E.S. Moss, A.M. Kammerer, J. Wu, J.M. Pestana, M.F. Riemer, R.B. Sancio, J.D. Bray, R.E. Kayen, and A. Faris, "Recent Advances in Soil Liquefaction Engineering: A Unified and Consistent Framework," 26th Annual ASCE Los Angeles Geotechnical Spring Seminar, Long Beach, CA, April 30, 2003.

Scott, C.R., *Soil Mechanics and Foundations*, Applied Science Publishers, Ltd., London, Second Edition, 1974.

Scott, G.A., J.T. Kottenstette, and J.F. Steighner, "Design and Analysis of Foundation Modifications for a Buttress Dam," *Proceedings, 38th U.S. Symposium on Rock Mechanics*, Washington, DC, A.A. Balkema, pp. 951-957, 2001.

Scott, G.A. "Probabilistic Stability Analysis – You Can Do It," Proceedings, Association of State Dam Safety Officials Conference, Austin, Texas, 2007.

Vick, S.G., *Degrees of Belief, Subjective Probability and Engineering Judgment*, ASCE Press, Reston, VA, 2002.

Watermeyer, C.F., "A Review of the Classical Method of Design of Medium Height Gravity Dams and Aspects of Base Shortening with Uplift," *Journal of the South African Institution of Civil Engineering*, Vol 48 No 3, pp. 2-11, 2006.